FLUID FLOW INVOLVING SLAG AND LIQUID STEEL IN AC ELECTRIC ARC FURNACES[1]

Y. I. C. Guzmán[2]
M. A. Ramírez-Argáez[3]
A. N. Conejo[2]
G. M. Trápaga[4]

Abstract
A mathematical model describing fluid flow for an industrial three phase Electric Arc Furnace has been developed which involves two immiscible liquids in the computational domain and the main driving force for the movement is due to buoyancy forces. Comparison between the case where only liquid steel occupies the entire computational domain and the case of two phases has been also carried out. The influence of slag physical and thermal properties on fluid flow and heat transfer is included in this work. The results of this work provide a clear description of flow patterns in the presence of the top slag layer. It has been found a marked effect of the slag phase to decrease the velocity patterns of liquid steel.
Key words: Fluid flow; Liquid steel; EAF.

[1] *Technical Contribution to the 40th Steelmaking Seminar – International, May, 24th-27th 2009, São Paulo, SP, Brazil.*
[2] Graduate program in metallurgy at *Morelia Technological Institute, Av. Tecnológico 1500, Morelia México. anconejo@gmail.com*
[3] *Metallurgical Engineering Department of the National Autonomous University of Mexico. México city.*
[4] *CINVESTAV-IPN Campus Queretaro. Queretaro-México.*

1 INTRODUCTION

Steel production through Electric Arc Furnaces (EAF) has been gaining acceptance over the last decades since this process can be part of both integrated plants and mini mills. Raw materials charged to this furnace range from scrap to Direct Reduced Iron (DRI). In order to increase the productivity and reduce the operational cost to produce steel in the EAF, electric energy consumption, tap to tap time and electrode consumption need to be reduced to a minimum level. Several technological improvements achieved in the EAF (most of them applied semi empirically) have addressed these reductions, but it remains the need to further improve the EAF performance. Foaming slag, ultrahigh power EAF, oxygen injection through lances, etc. are some of these improvements, however, it results evident that only fundamental understanding of the phenomena that govern the process efficiency of EAF will further improve the efficiency of the EAF.

A proper representation of the process through mathematical modeling may be a very valuable tool for a process engineer to be used to understand, control and optimize the process. However, its complexity makes it very difficult to include all phenomena taking place into the furnace. The model must contain basic features, such as electric arcs burning between the graphite cathodes (three of them in an alternate current EAF, AC-EAF) and the bath. The arcs are the main source of power needed to melt and heat the charge. Consequently, heat transfer is very important in this furnace, furthermore, since the molten metal is a fluid, convection rather than conduction heat transfer is more important, so turbulent fluid flow needs to be considered as a key phenomenon. Complexity increases because the bath is not composed only of liquid steel but liquid slag is also present. A two-liquid phase system is the real bath in an industrial EAF (without considering gases coming up from carbon oxidation during oxygen injection). If features such as foaming slag formation, or oxygen lancing are considered in the system, the resulting complexity is far beyond the current modeling capabilities.

There are no fundamental models reported so far that represents realistically the whole operation of an EAF. However, isolated phenomena have been modeled. DC-EAF mathematical model representations based on conservation equations have proposed by Ushio, Szekely e Chang[1] McKelliget and Szekely[2] and by Alexis et. al.[3] AC electric arcs have been fully described in a simpler way by the so called “Channel Arc Model” (CAM).[4] The coupling between the arcs and the steel bath have been modeled by Szekely, McKelliget e Choudhary[5] Ramirez et al.,[6] Kurimoto, Mondal e Morisue[7] and others but they represented the bath region to be a single steel phase in a very simple cylindrical crucible for both DC and AC systems. A two phase model steel – slag has not been proposed for a realistic EAF bath.

One previous investigation[8] has been reported for the EAF for a two-phase flow configuration which includes the top slag layer, in contrast to both the ladle furnace[9-12] and tundish.[13,14] Ramirez[8] as well as Nakajima (in ref 12) have reported that the top slag layer decreases the velocity in the liquid steel. Ramírez used a simple cylindrical geometry and conducted the analysis for 2D in rectangular coordinates. Jönsson et. al.[9-11] proved the importance of the top layer slag to obtain better predictions of experimental data in the ladle furnace. However, “numerical diffusion” or “false diffusion” was present in their computations with the inconvenient of a poor description of the sharp interface between steel and the slag. Ilegbusi et.al.[12] have also investigated the role played by the top slag layer during argon injection in the ladle furnace, however, they used a simple cylindrical geometry and the real two-

phase interaction considered was between liquid steel and gas bubbles. Simulations in continuous casting tundishes[13] of a two phase steel-slag system and in continuous casting molds[14] have also been reported using the Volume of Fluid (VOF) algorithm.
As a first approach a two liquid phase (steel/slag) bath flow driven by natural convection and heated by electric arcs in 3D for an industrial electric arc furnace is presented in this paper. The model was used to understand the effect of the slag and its physical properties on the heat transfer and fluid flow in an EAF bath. Such a model has not been reported yet and it may represent the starting point to describe very complex phenomena such as melting of DRI.

2 MATHEMATICAL MODEL

The model developed consists in describing the two phase fluid flow driven by natural convection and heated by electric arcs that in turn were described by the CAM approach.

The CAM Approach

The CAM was applied to a 3 phase AC-EAF, and its formulation may be found elsewhere.[4] The idea behind the model is a simple energy balance in which the electric power of the arc generated by the Joule effect is dissipated to its neighborhood through radiation, convection and electric flow. The model assumes that the arc has a uniform temperature and the shape of a cylinder. The current – voltage dependency is described by assuming that the three phase electric circuit behaves symmetrically. Physical properties of the plasma air in the arc which is above 10,000K are taken from Murphy.[15] Electric parameters of an industrial furnace to be feed into the model are presented in Table 1. Mathematically, the model consists in several ordinary differential equations that were numerically solved by the 4º order Runge-Kutta algorithm which was written in a visual basic subroutine. This model is needed to determine the amount of heat flow that is transferred from the arc to the bath and this flow entering at the free surface of the EAF bath is set as a boundary condition in the bath model.

Table 1. Electric parameters of an industrial arc used to simulate the arc region with the Channel Arc Model

Gas	**Air**
Surroundings temperature	*1100 K*
Cathode current density	$4.4x10^7\ A/m^2$
Anode work function	*4.75 V*
Anode voltage drop	*5.0 V*
Cathode voltage drop	*5.0 V*
Electric Resistance	$0.412\ m\Omega$
Inductance	$3.79\ \mu H$
Transformer Voltage	*1937.5V*
Frequency	*60 Hz*

The Bath Model

An industrial crucible of an EAF was drawn and divided in 93534 nodes to form a structured grid. At any position the sum of the volume fractions of both phases must

be unity. Physical properties of the fluid are assigned according to the values of the volume fractions. Locations where the steel volume fraction is 1, steel properties are set and those locations with a 0 value of the steel volume fraction will take those for the slag properties. At positions where the steel volume fraction ranges between 0 or 1, physical properties are the weighted sum depending on the values of the volume fraction.

Assumptions:
Important assumptions are that the free surface is flat, constant physical properties of slag and steel and the flow is only driven by natural convection in a three phase EAF bath. Foaming slag and oxygen lancing are not taken into account.

Governing equations
The governing equations correspond to the conservation of energy, momentum and mass. The algorithm MIXTURE (16-17) included in the commercial computational code FLUENT is used to describe multiphase flow. In this algorithm the continuity and momentum equations are written for the mixture, the volume fraction equation for the secondary phase and an algebraic expression for the relative velocity.

Mass conservation (continuity) for a fluid of constant density:

$$\frac{\partial}{\partial t}(\rho_m) + \nabla \bullet (\rho_m u_m) = 0 \tag{1}$$

Where: ρ_m is the density of the mixture and u_m the average mass velocity. They are defined by the following expressions.

$$\rho_m = \sum_{i=1}^{2} r_i \rho_i \tag{2}$$

$$\bar{u}_m = \frac{\sum_{i=1}^{2} r_i \rho_i u_i}{\rho_m} \tag{3}$$

r_i is the volume fraction of each phase (steel and slag).

Momentum conservation
Momentum conservation is defined by the following general expression.

$$\frac{\partial}{\partial t}(\rho_m u_m) + \nabla \cdot (\rho_m u_m u_m) = -\nabla \cdot P + \nabla \cdot \left[\mu_m \left(\nabla u_m + \nabla u_m^T\right)\right] + \rho_m \bar{g} + F \tag{4}$$

μ_m represents the viscosity of the mixture, computed as follows.

$$\mu_m = \sum_{i=1}^{2} r_i \mu_i \tag{5}$$

Thermal energy conservation
For a fluid at constant pressure, density independent of temperature and any number of phases, the thermal balance is given by the following expression

$$\frac{\partial}{\partial t}\sum_{i=1}^{2}\left(r_i\rho_i T_i\right)+\nabla\cdot\sum_{i=1}^{2}r_i u_i\left(\rho_i T_i\right)=\nabla\cdot\left(\frac{k_{eff}}{cp_i}\nabla T_i\right)+S_i \tag{6}$$

where k_{eff} is the effective thermal conductivity.

$$k_{eff}=\sum_{i=1}^{2}r_i\left(k_{li}+k_{ti}\right) \tag{7}$$

k_{li} and k_{ti} are the laminar and turbulent thermal conductivity, respectively.

The standard k-ε turbulence model is employed in this work.

Boundary conditions:

Since transient calculations were computed, initial conditions needed to be set.

Velocities: Boundary conditions at the bottom and lateral walls represent zero turbulence and non-slip boundary conditions, i.e. zero velocities, are imposed at the furnace walls. Zero shear stresses, τ_{zy}, at the steel surface are possible by ignoring two driving forces; electromagnetic body forces and shear forces from the arc.

$$\tau_{zy}=-\mu_{eff}\frac{dv_y}{dz}=0\,;\quad @\ -R\le x\le R;\ -R\le y\le R;\ z=H \tag{8}$$

Where: R represents the radius of the furnace and H the height of liquid steel.

Fluid flow at the top boundary is a flat free surface where slip of the top phase is allowed (slag).

Heat input: For a given set of electric parameters (voltage and arc length), power delivery (P_o) represents a constant heat input, as indicated below.

$$-k_{eff}\frac{\partial T}{\partial z}=P_o \tag{9}$$

P_o is computed by the Channel Arc Model (CAM). A value of 120 MW results when the power system operates at 1210 volts and 45 cm in arc length.

Additionally radiation heat exchange between the surface and the surroundings is also taken into account.

$$Q_{cam}=\lambda k_b\left(T_a^4-T_s^4\right) \tag{10}$$

Where: λ is the emissivity of the slag (0.8), k_b is the Stefan–Boltzmann´s constant T_s is the slag surface temperature, which changes as a function of position and time, and T_a is the ambient temperature,

Heat losses through the walls are computed using Fourier´s law.

$$Q_{walls}=-k_{MgO}\frac{dT}{dx} \tag{11}$$

The magnitude of this thermal losses yield 5937 Wm^{-2} considering a furnace wall of 45 cm, inner temperature of 1600°C, outer temperature of 200°C and a thermal conductivity for MgO of 1.9 $Wm^{-1}K^{-1}$.

Steel physical properties are considered constant and provided in Table 2. Since one of the objectives of this work is to study the effect of the slag properties on the fluidynamics and heat transfer of a AC-EAF. Then, a process analysis was conducting varying some of the most important properties of the slag. These properties depend on the temperature but also on the chemical compositions of the slag which may vary dramatically depending on the oxidizing conditions prevailing in the furnace. The amount of FeO in the slag increases if the furnace operates under oxidizing conditions. Table 2 also shows values of the ranges of the physical properties of the slag used in this work and other bath conditions required for the simulations.

Table 2. Steel and slag physical properties and bath conditions for simulations.

Layer of slag	h = 35 cm
Arc length and electric power of the arc	H = 45 cm, 120.6 MW
Slag density @ 1873 K	3000 kg / m^3
Slag viscosity range @ 1873 K	0.05 – 0.45 kg/ms (standard value of 0.1 kg/ms)
Slag thermal conductivity range @ 1873 K	0.1 – 6.3 W/mK 0.2 (standard value of 1.2 W/mK)
Slag specific heat @ 1873 K	1170 J / kg K
Slag thermal expansion coefficient @ 1873 K	0.00027 K^{-1}
Steel density @ 1873 K	7200 kg / m^3
Steel viscosity @ 1873 K	0.0065 kg / m s
Steel thermal conductivity @ 1873 K	15 W / m K
Steel specific heat @ 1873 K	670 J / kg K
Steel thermal expansion coefficient @ 1873 K	0.00014 K^{-1}

Solution

Solution of the conservation equations was done by the finite element method which is built in the commercial fluid dynamics code FLUENT. Solution of each case took around 15 hours of computer time by performing transient calculations to reach 200 seconds in real time. The grid was chosen after a grid sensibility analysis with 4 different meshes.

3 RESULTS AND DISCUSSION

Figure 1 shows the computational domain with three electrodes supplying a total arc power of 120.6 MW, which results from tap settings at 1210 volts and 45 cm of arc length. This industrial furnace has a nominal capacity of 220 tons of liquid steel, equipped with EBT facilities.

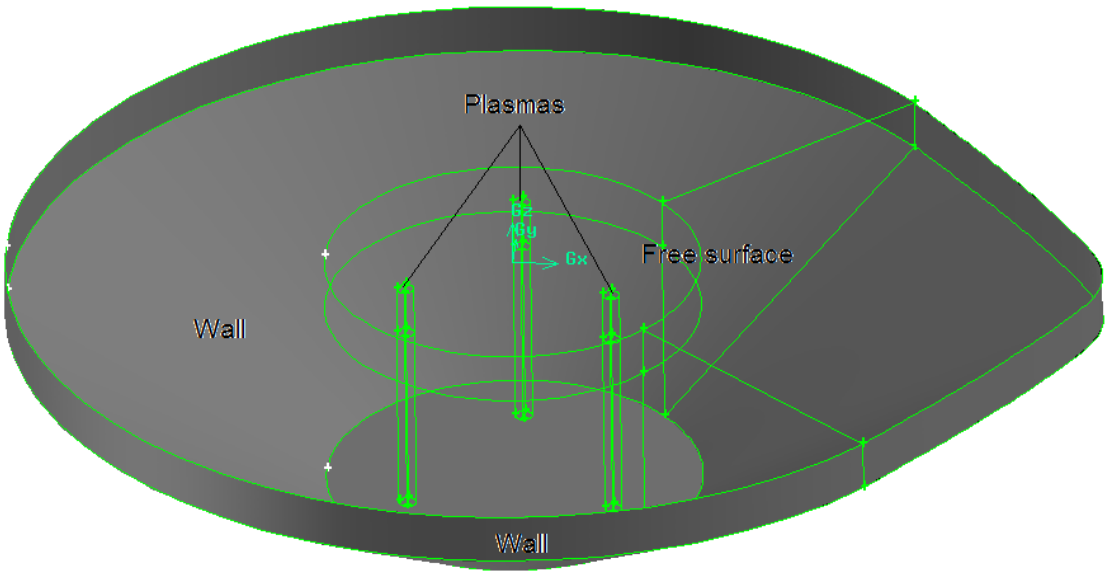

Figure 1. Computational domain of the industrial EAF

Flow and Temperature Anatomy of the EAF Bath

Figure 2 shows the resulting fluid flow velocity vectors of the entire AC-EAF bath after 200 seconds during the heat. Three planes are depicted in the same figure. These planes are depicted in more detail in Figures 3 and 4. Figure 3 shows the cross sectional plane A-B and close-ups of two regions within the planes A-B and C-D. Each fluid element below the pitch circle is heated by the electric arcs and thus decreasing its density. Motion of this fluid occurs due to density gradients across the planes parallel to the free surface. Hot liquid at the center and colder liquid at the walls yield different densities in the presence of a gravitational field, driving the more dense fluid elements to the bottom. This phenomenon is repeated at each plane, explaining an apparent abnormal behavior in case fluid flow is analyzed in the vertical direction. In this direction, all fluid elements at the bottom are colder and with higher density, in spite of this, they move upwards replacing fluid elements at higher temperatures of lower density. The final result is the formation of two circulation loops with liquid ascending in the center of the furnace and descending at the furnace walls. Slag on top of the steel also shows the same two circulations loops in the same flow pattern as the steel but since the slag layer is shallow these circulations present a higher radial momentum than those of the steel. The average velocity of the two phase flow is approximately 2 cms^{-1}. Sections (b) and (c) in this figure describe in full detail the flow patterns of both steel and liquid slag. It is clearly observed how the velocity vectors of the two liquid phases point in opposite directions at the slag-liquid interface. Since the two liquid phases are moving in opposite directions at the interface, the negative momentum exchange (friction) is very high between the slag and the steel, and the former phase slows down while loses momentum at the slag-steel interface. This behavior is a clear explanation to the observed phenomena of flow retardation and less agitation due to the presence of the slag phase.

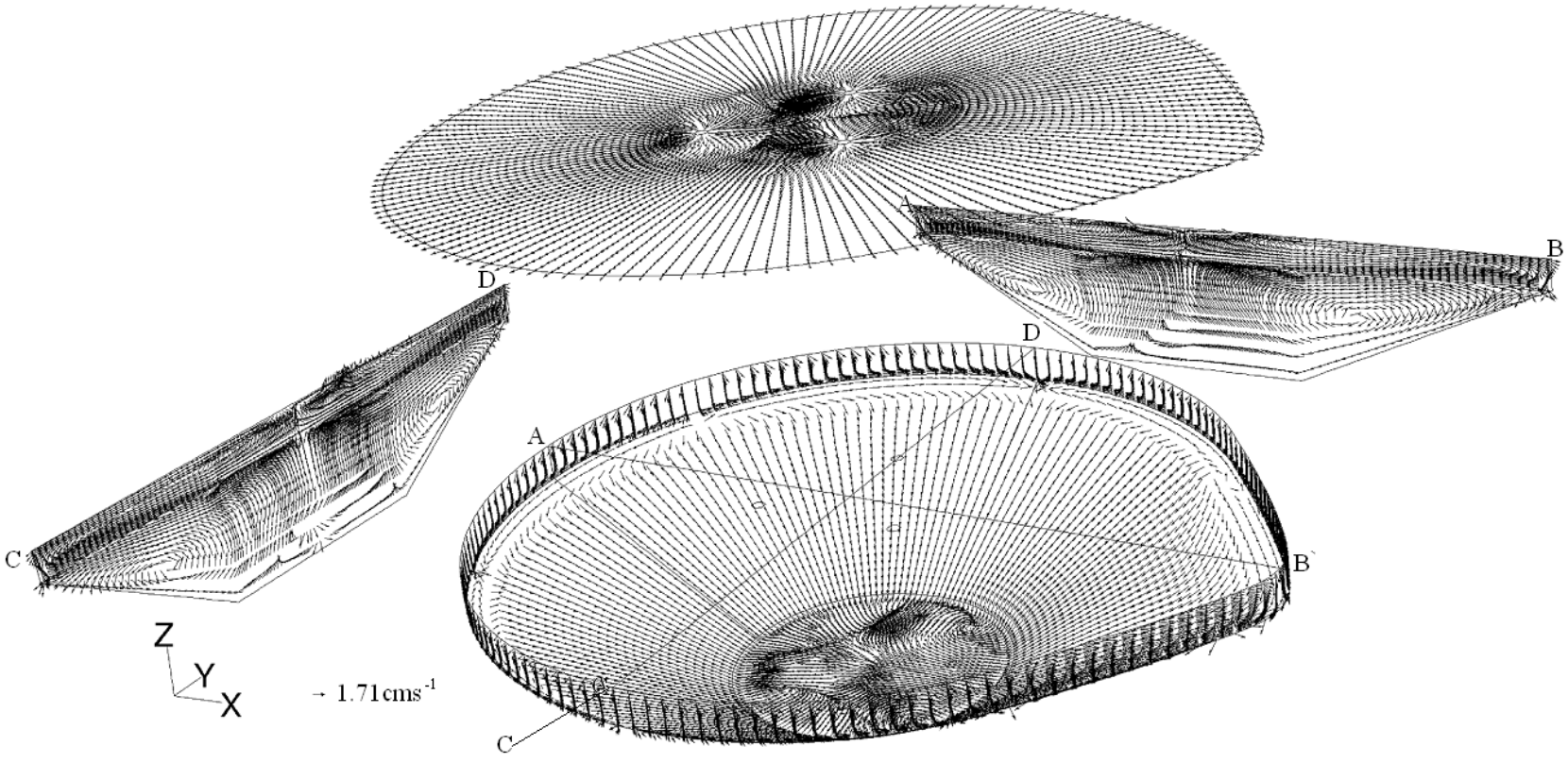

Figure 2. Velocity fields in the entire computational domain

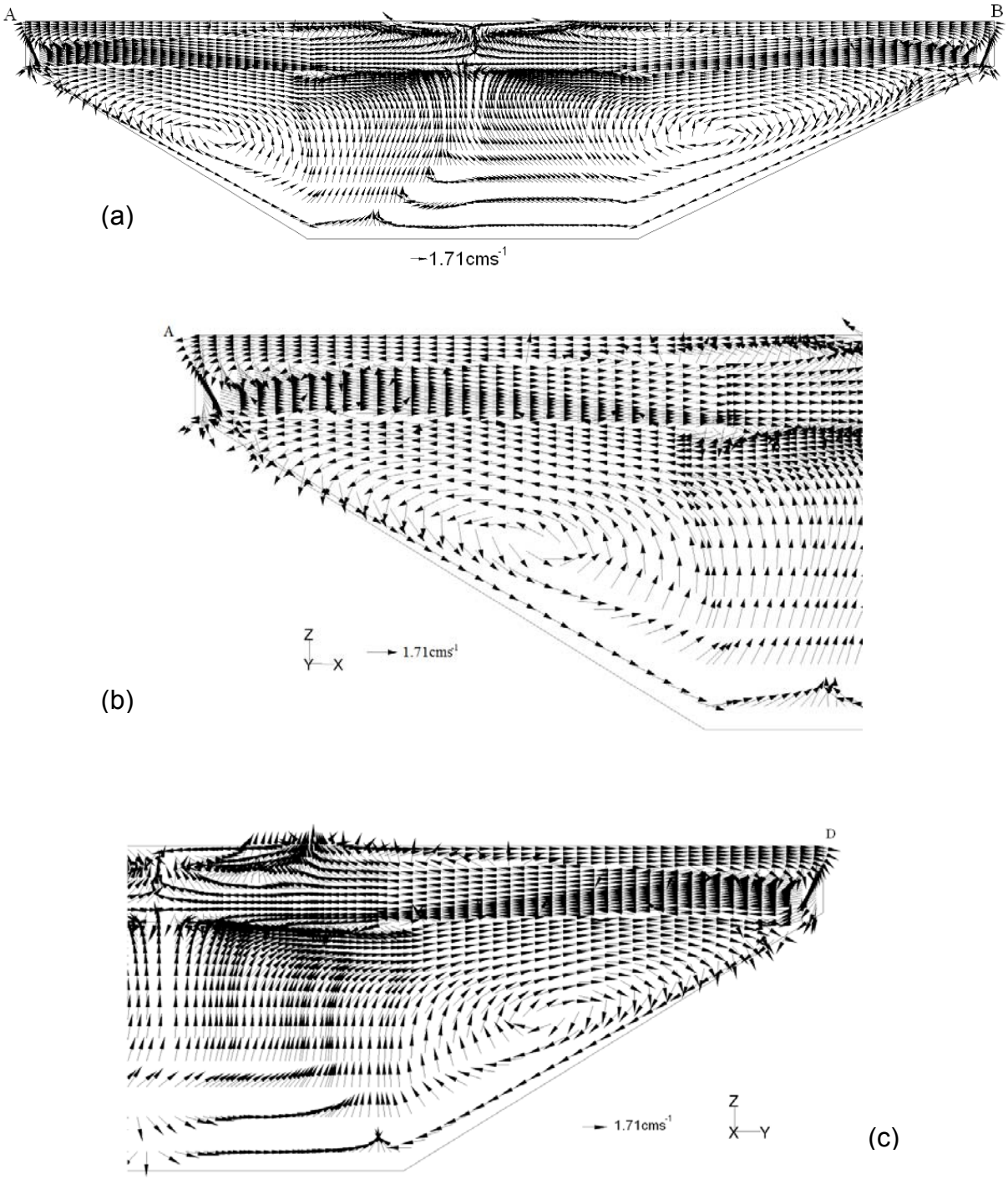

Figure 3. Velocity fields. (a) for the cross sectional plane AB (b) detail plane AB and (c) detail plane CD

Figure 4, a top view, shows fluid flow from the liquid surrounding the three electrodes. Circulation loops depicted in the liquid steel can be explained in a similar way: since the steel is hotter in the middle of the furnace, this less dense liquid goes up while the more dense cold steel close to the walls goes down causing the two circulation loops in the steel.

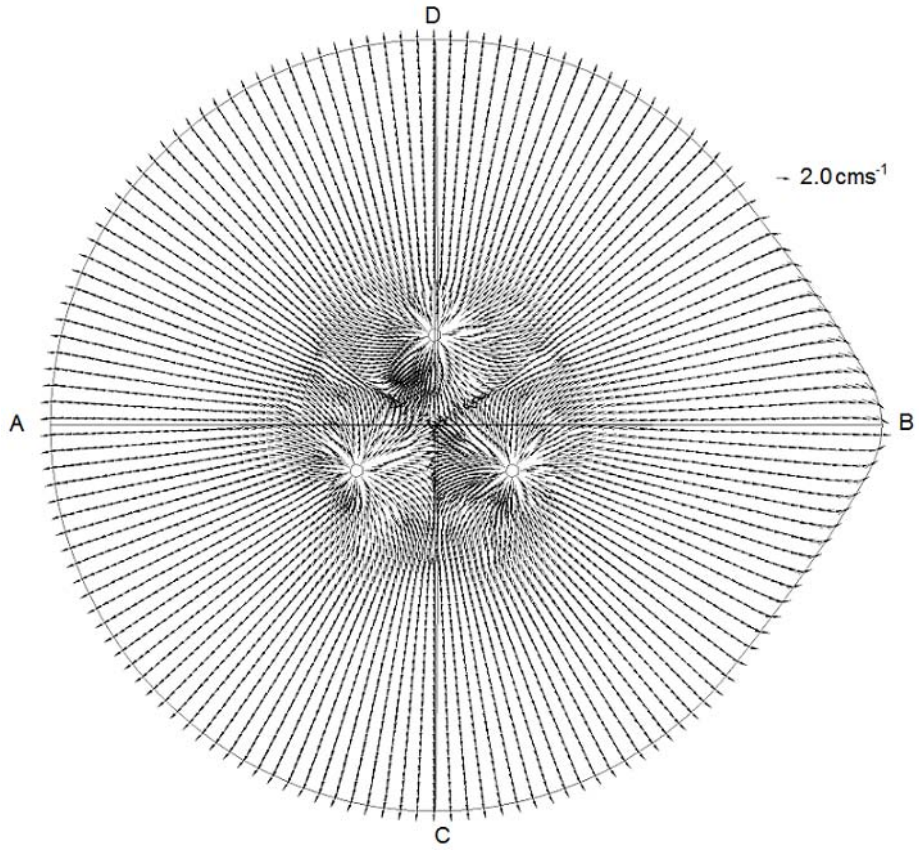

Figure 4. Free surface describing velocity fields around the three electrodes

Figure 5 shows temperature contours at the same time of 200 seconds. High temperatures are on the free surface at the three arc attached zones (pitch circle) and as distance from the arc increases bath temperature of the slag and steel decreases. Temperature gradients are also bigger at the free surface and as the depth increases temperature gradients also decrease. Temperature stratification is bigger in the slag than in the steel that has a more uniform temperature because the thermal conductivity of the metal is higher than the slag. Fluid flow patterns are explained with the help of the temperature contours. Once the hot fluid moving in a radial direction reaches the wall then goes down and returns to the arc zones since below is an immiscible phase.

Effect of the Slag on Fluid Flow

In order to determine the effect of the top slag layer on the fluid dynamics of a EAF bath, two simulations were compared; a single steel phase and a two-phase system (liquid steel – slag), with the same geometry and boundary conditions but varying the arc length. Figure 6 shows the average velocity of the entire system in both computations. It is clearly seen that under the same heating conditions, steel phase alone moves faster than when it has on the top a slag layer. The slag acts as a buffer that reduces the momentum transfer in the steel. Friction between the steel and the slag (a more viscous phase) reduces steel motion when compared to the case where steel moves freely in a frictionless atmosphere. On average the velocity of liquid steel decreases from 5 cms^{-1} to 2 cms^{-1} due to the presence of the top slag phase.

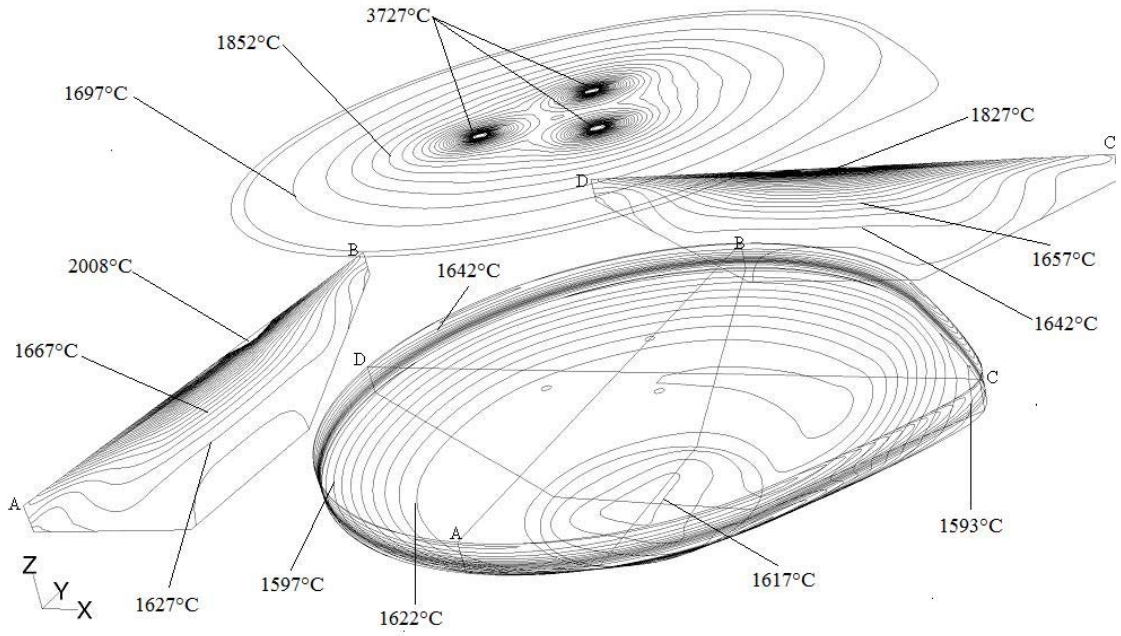

Figure 5. Temperature contours in the EAF

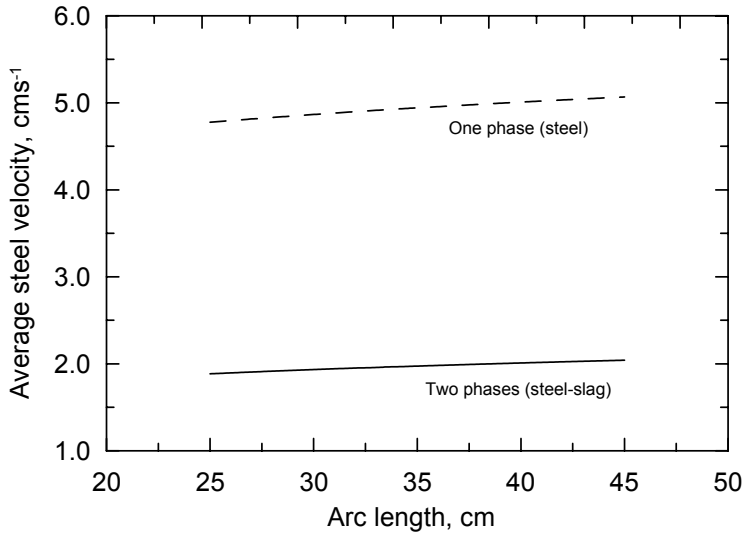

Figure 6. Comparison of velocities in a one and a two phase system

Effect of slag viscosity on heat transfer and fludynamics

Figures 7 and 8 show the average velocity and temperature of the whole EAF bath, respectively, as a function of the slag viscosity. The heating was provided by an arc operating at 1210V, 45cm of arc length that provides 120.6 MW. The layer of slag was kept at 35cm and the averages where taken at 200 seconds of heating. As the slag viscosity increases velocities decrease but temperatures increase in the bath. A more viscous fluid will appose to be shear and will not flow easily and consequently its velocity decreases, as shown in Figure 8. Simultaneously, a more static fluid will transfer less heat by convection and consequently less heat is dissipated from the arc attached zones and the liquid gets hotter since can not dissipate heat through the surroundings and to the rest of the furnace, as shown in Figure 9. It is also expected more thermal stratification in the bath as the slag viscosity increases.

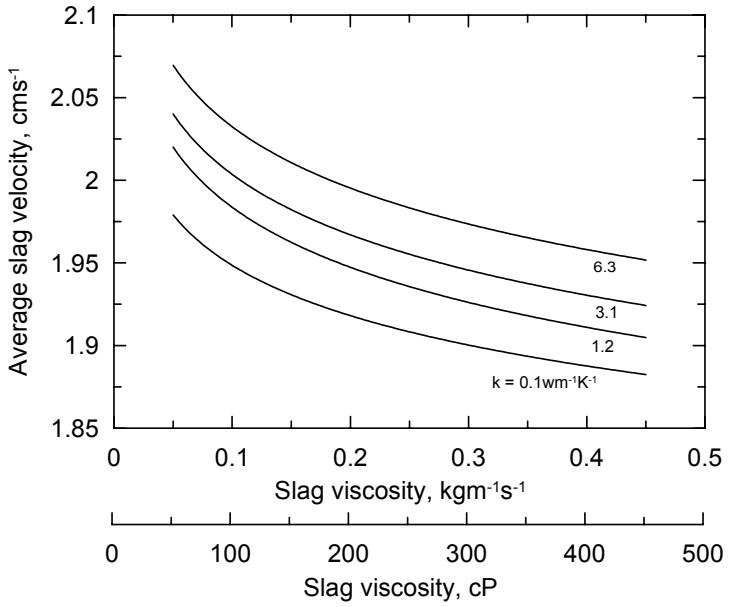

Figure 7. Effect of slag viscosity on its velocity

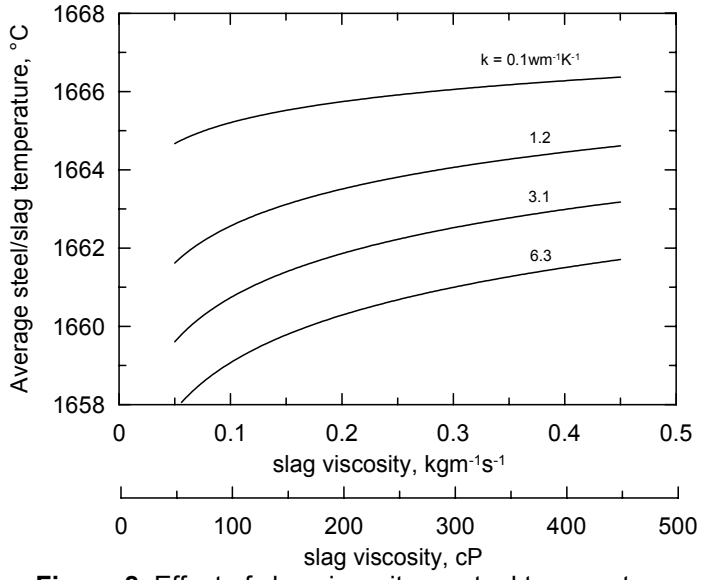

Figure 8. Effect of slag viscosity on steel temperature

Effect of slag thermal conductivity on heat transfer and fludynamics

Figures 9 and 10 show the average velocity and temperature of the whole EAF bath, respectively, as a function of the thermal conductivity of the slag. The heating was provided by an arc operating at 1210V, 45cm of arc length that provides 120.6 MW. The layer of slag was kept at 35cm and the averages where taken at 200 seconds of heating. As the thermal conductivity increases bath velocity slightly decreases and bath temperature slightly increases. As a matter of fact neither the velocity nor the temperature of the bath changes with thermal conductivity of the slag. What happens is that convection of the bath and turbulent diffusion are more important heat transfer mechanisms than pure conduction. Therefore, bath velocity and temperature are insensitive to a change in the thermal conductivity of the slag.

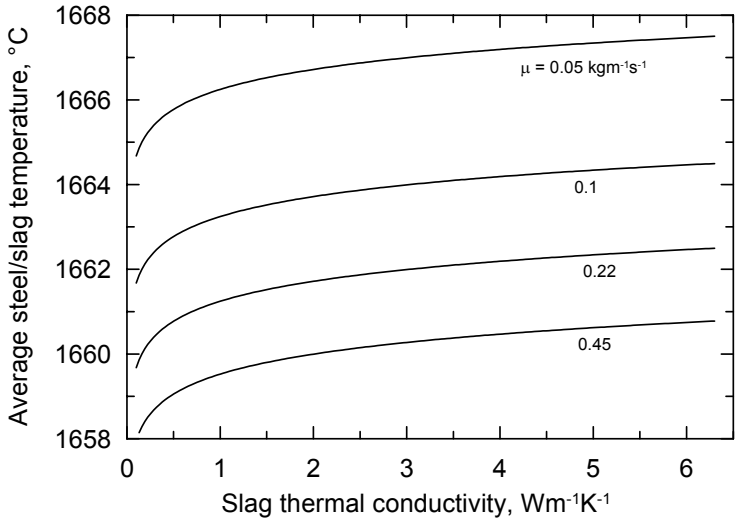

Figure 9. Effect of slag thermal conductivity on heat transfer

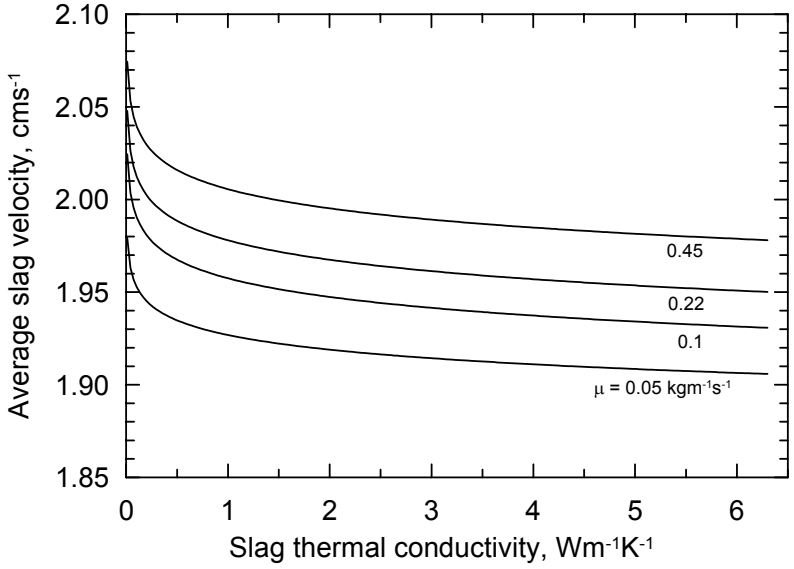

Figure 10. Effect of slag thermal conductivity on its velocity

4 CONCLUSION

A two liquid phase (steel-slag) mathematical model of an industrial AC-EAF bath was developed considering the heating of electric arcs, radiation exchange with surroundings at the free surface and natural convection. The CAM approach was used to represent the electric arc and the heat flow computed from this model was set as a boundary condition in the bath model solved by the Mixture algorithm built in FLUENT. The model is capable to predict the fluid flow patterns and temperature stratification of the slag and the steel phases. The main conclusions of this work are:

- Fluidynamics is governed by natural convection produced by the heating effect of the 3 electric arcs developed in a three phase EAF. Circulation loops are developed in the liquid slag starting at the arc attached zones and ending at the lateral walls of the furnace.
- The slag phase reduces the momentum of the liquid steel due to the friction between both phases. Therefore, steel will move freely and faster without a

top layer of slag. A decrease from 5 cms^{-1} to 2 cms^{-1} is due to the presence of the top slag phase

- As the slag viscosity increases (as a consequence of its chemical composition) convection in the EAF bath decreases and thermal stratification increases due to a more rigid liquid slag that flows slowly and dissipates less rapidly thermal energy.
- Thermal conductivity of the slag has a negligible effect on the heat transfer and fluid flow of a AC-EAF bath since convection and turbulent diffusion contribute more to the heat transfer than conduction.

REFERENCES

1 USHIO, M.; SZEKELY, J.; CHANG, C.W. Mathematical modeling of flow field and heat transfer in high-current arc discharge. *Ironmaking and Steelmaking*, v. 6, n. 1, p. 279-86, 1981.

2 McKELLIGET, J.; SZEKELY, J. A mathematical model of the cathode region of a high intensity carbon arc. J*. Phys. D: Appl. Phys*., v.16, p. 1007-22, 1983.

3 ALEXIS, J.; RAMIREZ, M.; TRAPAGA, G.; JONSSON, P. Modelling of a DC Electric Arc Furnace – Heat Tranfer From The Arc. *ISIJ International*, v. 40, n. 11, p. 1189-97, 2000.

4 LARSEN, H.L.; SAEVARSDOTTIR, G.; BAKKEN, J. A. simulation of AC arcs in the silicon metal furnace. In: ELECTRIC FURNACE CONFERENCE, 1996. p. 1-12.

5 SZEKELY, J.; McKELLIGET, J.; CHOUDHARY, M. Heat-transfer fluid flow and bath circulation in electric arc furnaces an DC plasma furnaces. *Ironmaking and steelmaking*, v. 3, n. 4, p.169-79. 1983.

6 RAMIREZ, M.; ALEXIS, J.; TRAPAGA, G.; JONSSON, P.; McKELLIGET, J. Modelling of the electric arc furnace – mixing in the bath. *ISIJ International*, v. 41, n. 10, p. 1146-55, 2001.

7 KURIMOTO, H.; MONDAL, H.N.; MORISUE, T. Analysis of velocity and temperature fields of molten metal in DC electric arc furnace. *Journal of Chemical Engineering of Japan*, v. 29, n. 1, p. 75-81, 1996.

8 RAMIREZ-ARGAEZ, M.A. PhD Thesis, MIT, Metallurgy department. Boston MA USA, 2000.

9 JONSSON, L.; JONSSON, P. Modeling of the fluid conditions around the slag metal interface in a gas-stirred ladle. *ISIJ International*, v. 36, n. 9, p. 1127-34, 1996.

10 JONSSON, L.; SICHEN, D.; JONSSON, P. A new approach to model sulphur refining in a gas-stirred ladle- A coupled CFD and thermodynamic model. *ISIJ International,* v. 38,n. 3, p. 260-7, 1998.

11 ANDERSSON, M.A.T.; JONSSON, L.T.I.; JONSSON P. A thermodynamic and kinetic model of reoxidation and desulphurization in the ladle furnace. *ISIJ International*, v. 40, n. 11, p. 1080-8, 2000.

12 ILLEGBUSI, O.J.; IGUCHI, M.; NAKAJIMA, K.; SANO, M.; SAKAMOTO, M. Modeling mean flow and turbulence characteristics in gas-agitated bath with top layer. *Metallurgical and Materials Transactions B*, v. 29, p. 211-22, Feb. 1998.

13 SOLHED, H.; JONSSON, L.; JONSSON, P. Modeling of the steel/slag interface in a continuous casting tundish. *Steel Research International*, v. 79, n. 5, p. 348-57, 2008.

14 YU, H.; ZHU, M. The interfacial behavior of molten steel and liquid slag in slab continuous casting mold with electromagnetic brake and argon gas injection. *Acta Metallurgica Sinica*, v. 44, n. 9, p. 1141-8, 2008.

15 MURPHY, A.B. Transport coefficients of air, argon-air and oxygen-air plasmas. *Plasma Chemistry and Plasma Processing*, v. 15, n. 2, p. 279-307, 1995.

16 FLUENT User's Guide (version 6.2). Documentation. 2005. Fluent incorporated.

17 MANNINEN, M.; TAIVASSALO, V.; KALLIO, S. On the mixture model for multiphase flow. [S.l.]: Technical Research Centre of Finland, 1996. (VTT Publications, 288).